ISME

www.nature.com/ismecomms

ARTICLE OPEN

Changes in the membrane lipid composition of a *Sulfurimonas* species depend on the electron acceptor used for sulfur oxidation

Su Ding[1✉], Jan V. Henkel[2,3], Ellen C. Hopmans[1], Nicole J. Bale[1], Michel Koenen[1], Laura Villanueva[1,4] and Jaap S. Sinninghe Damsté[1,4]

Sulfurimonas species are among the most abundant sulfur-oxidizing bacteria in the marine environment. They are capable of using different electron acceptors, this metabolic flexibility is favorable for their niche adaptation in redoxclines. When oxygen is depleted, most *Sulfurimonas* spp. (e.g., *Sulfurimonas gotlandica*) use nitrate (NO_3^-) as an electron acceptor to oxidize sulfur, including sulfide (HS^-), S^0 and thiosulfate, for energy production. *Candidatus* Sulfurimonas marisnigri SoZ1 and *Candidatus* Sulfurimonas baltica GD2, recently isolated from the redoxclines of the Black Sea and Baltic Sea respectively, have been shown to use manganese dioxide (MnO_2) rather than NO_3^- for sulfur oxidation. The use of different electron acceptors is also dependent on differences in the electron transport chains embedded in the cellular membrane, therefore changes in the membrane, including its lipid composition, are expected but are so far unexplored. Here, we used untargeted lipidomic analysis to reveal changes in the composition of the lipidomes of three representative *Sulfurimonas* species grown using either NO_3^- and MnO_2. We found that all *Sulfurimonas* spp. produce a series of novel phosphatidyldiazoalkyl-diacylglycerol lipids. *Ca.* Sulfurimonas baltica GD2 adapts its membrane lipid composition depending on the electron acceptors it utilizes for growth and survival. When carrying out MnO_2-dependent sulfur oxidation, the novel phosphatidyldiazoalkyl-diacylglycerol headgroup comprises shorter alkyl moieties than when sulfur oxidation is NO_3^--dependent. This is the first report of membrane lipid adaptation when an organism is grown with different electron acceptors. We suggest novel diazoalkyl lipids have the potential to be used as a biomarker for different conditions in redox-stratified systems.

ISME Communications; https://doi.org/10.1038/s43705-022-00207-3

INTRODUCTION

Chemoautotrophic bacteria of the genus *Sulfurimonas* [class Campylobacterota, according to the NCBI classification, [1, 2] play an important role in sulfur oxidation in sulfidic habitats, such as stratified marine waters, anoxic sediments, and hydrothermal deep-sea vents, as well as in some terrestrial environments [3]. For example, along the Namibian shelf, Lavik, et al. [4] reported that occasionally occurring, large-scale sulfidic water masses were detoxified by oxidation of sulfide (HS^-) using nitrate (NO_3^-) by two groups of bacteria: *Sulfurimonas* spp. and bacteria falling in the gammaproteobacterial sulfur oxidizer cluster. Within and below the pelagic redoxcline of the Baltic Sea, where a stable redoxcline separates deep anoxic sulfidic water from oxygenated surface water [5], *Sulfurimonas* spp. accounted for up to 15% of total prokaryotic abundance. Here, Grote, et al. [6] isolated *S. gotlandica* GD1^T, a denitrifying chemolithotrophic sulfide oxidizer. In oxygen deficient systems, sulfur cycling has been shown to be tightly linked to the nitrogen cycle without affecting chemical gradients, so called cryptic cycling [e.g., [7, 8].

In the stratified water columns of both the Baltic Sea and the Black Sea, NO_3^- and nitrite (NO_2^-) often disappear before the first appearance of HS^- [9, 10]. Geochemical water column profiles suggest that extensive cycling of dissolved and particulate manganese (Mn) may quantitatively account for the oxidation of HS^-, thereby shuttling oxidative potential of O_2 and NO_3^- over several meters distance. This mechanism, as well as a potential biological catalyzation, was proposed earlier because chemoautotrophic HS^- oxidation could not be linked to O_2 or NO_3^- [10–12]. Recently, Henkel, et al. [13] isolated *Ca.* Sulfurimonas marisnigri SoZ1 from the redoxcline of the central Black Sea. This bacterium can couple the oxidation of reduced sulfur compounds, including HS^-, S^0 and thiosulfate, to the reduction of MnO_2. The biologically catalyzed oxidation of HS^- by *Ca.* S. marisnigri SoZ1 is faster than the abiotic oxidation of HS^- with MnO_2 [14] and yields SO_4^{2-} as the prominent end product, while elemental sulfur (S^0) accumulates in the abiotic reaction [13, 15, 16]. Combining the cellular abundance of *Sulfurimonas* spp. in the Black Sea redoxcline with rates of MnO_2 dependent HS^- oxidation by *Ca.* S. marisnigri SoZ1 in a reaction diffusion

[1]NIOZ Royal Institute for Sea Research, Department of Marine Microbiology and Biogeochemistry, Texel, The Netherlands. [2]Department of Bioscience, Center for Geomicrobiology, Aarhus University, Aarhus, Denmark. [3]Biological Oceanography, Leibniz Institute for Baltic Sea Research Warnemünde, Rostock, Germany. [4]Department of Earth Sciences, Faculty of Geosciences, Utrecht University, Utrecht, The Netherlands. ✉email: su.ding@nioz.nl

Received: 11 July 2022 Revised: 5 December 2022 Accepted: 13 December 2022
Published online: 24 December 2022

model yielded adequate rates to counterbalance the HS^- flux, resulting in the measured HS^- concentration profile, in contrast to a pure abiotic reaction [14]. Hence, this process is likely to play a prominent role in HS^- oxidation at the chemocline of the Black Sea. Likewise, *Ca*. Sulfurimonas baltica GD2 was isolated from the redoxcline of the Gotland Deep in the Baltic Sea [17]. These studies revealed the important role of MnO_2-dependent *Sulfurimonas* spp. in biogeochemical cycling in redox-stratified systems [14]. Changes in the electron acceptor are associated with differences in the electron transport chain (ETC), which is embedded in the cellular membrane. Protein complexes of the ETC are expected to interact with and influence the lipid composition of the membrane, which is partially responsible for the fluidity of the membrane [18]. Nevertheless, few studies have addressed potential changes in the membrane lipid composition upon changes in the electron acceptor as a response to maintain the cell homeostasis.

Structurally diverse microbial lipids play important roles as the building blocks of membranes and play a role in energy storage, signaling and modulation of protein activity [19]. Many microorganisms maintain their membrane functionality, permeability, and fluidity during changing environmental conditions by membrane adaptation [20, 21] through the regulation of its lipid composition [e.g., [22–25]. For instance, when phosphorus is limited, phytoplankton and some bacteria can use non-phosphorus lipids to replace phospholipids for survival [23, 26, 27]. However, the membrane lipid composition of *Sulfurimonas* spp., and potential differences when using different electron acceptors to oxidize HS^-, are unknown. Until now, only a few studies have reported the predominant cellular fatty acids of *Sulfurimonas* spp. [e.g., [28–30], but their intact polar lipid composition, including both the fatty acid side chain and their linked polar headgroups, remains to be studied. Because of their relatively high abundance in redox-stratified waters, *Sulfurimonas* spp. are likely to contribute substantially to the lipidome of these environments. Recent advances in the field of lipidomics, using non-targeted approaches combined with computational methods, allows for comprehensive lipidome profiling [31–34].

Here, we examined the lipidome of three *Sulfurimonas* species, *S. gotlandica* GD1^T and *Ca. S.* baltica GD2, both isolated from water column of the Baltic Sea, and *Ca. S.* marisnigri SoZ1 isolated from the water column of the Black Sea, cultured with either NO_3^- or MnO_2 as electron acceptor. Our aim was to investigate how *Sulfurimonas* spp. adjust their membrane lipid composition when using different electron acceptors (NO_3^- and MnO_2), in order to determine potential microbial adaptations of the membrane linked to different metabolisms.

METHODS AND MATERIALS

Cultures

Anoxic medium was prepared with a salinity of 21, 14 and 10 psu for *Ca*. S. marisnigri SoZ1, *Ca*. S. baltica GD2 and *S. gotlandica* GD1^T respectively as described before [17] with minor changes. We used 2 L glass bottles closed with butyl rubber stoppers for both MnO_2 and NO_3^- conditions with Ca. S. marisnigri SoZ1 and Ca. S. baltica GD2. S. gotlandica was cultivated in 100 mL serum bottles closed with butyl rubber stoppers. We raised the concentration of NH_4Cl and Na_2HPO_4 from 0.02 mM and 0.01 mM to 2.5 mM and 0.2 mM, respectively. These adjustments were made to exclude deficiencies of macro nutrients during growth and should therefore reduce differences in lipid composition of cultures. Cultures were obtained from the internal culture collection of the IOW, which are also available at the German Collection of Microorganisms and Cell Cultures GmbH (DSMZ) and at the Japan Collection of Microorganisms (JCM) with the identifiers JCM 39139 and DSM 111879 (*Ca*. S. marisnigri SoZ1), JCM 39138 and DSM 111898 (*Ca*. S. baltica GD2) and JCM16533 and DSM 19862 (*S. gotlandica* GD1^T). *Ca*. S. marisnigri SoZ1 and *Ca*. S. baltica GD2 were cultured with either 3 mM thiosulfate ($S_2O_3^{2-}$) and 5 mM MnO_2 (Mn-reducing conditions) or 5 mM $S_2O_3^{2-}$ and 10 mM NO_3^- (NO_3^- reducing conditions). *S. gotlandica* GD1^T was amended with 15 mM NO_3^- and 10 mM $S_2O_3^{2-}$. *S. gotlandica* GD1 grows faster and has a substantially higher growth efficiency with nitrate than Ca. S. marisnigri SoZ1 and Ca. S. baltica GD2. This is because *S. gotlandica* GD1 is a complete denitrifier (NO_3^- to N_2), while Ca. S. marisnigri SoZ1 and Ca S. baltica GD2 can only reduce NO_3^- to NO_2^- [17]. Since *S. gotlandica* grows faster than the other strains, the initial NO_3^- and $S_2O_3^{2-}$ concentrations were higher to prolong the exponential growth phase. Concentrations of NO_3^- (and therefore also $S_2O_3^{2-}$) in cultivations of Ca. S. marisnigri SoZ1 and Ca. S. baltica GD2 are lower to exclude a putative toxification by NO_2^-. Cell numbers were estimated after 8 days of growth and the biomass were harvested at day 12 at 10 °C in the dark. Cellular abundance of *Ca*. S. marisnigri SoZ1 and *Ca*. S. baltica GD2 were ~5×10^6 cells mL^{-1} under Mn-reducing conditions and ~5×10^5 cells mL^{-1} under NO_3^- reducing conditions (*Ca*. S. baltica GD2 only). Very few cells were visible under NO_3^- reducing conditions with *Ca*. S. marisnigri SoZ1. *S. gotlandica* GD1^T reached a cellular abundance of ~4×10^7 cells mL^{-1} at day 8. Incubation was continued until day 10 at which the black color of Mn-containing incubations became slightly brownish-gray, indicating the precipitation of Ca-rich Mn-carbonates at the end of the exponential growth phase [13, 17]. Cells were harvested in 50 mL centrifugation tubes at 4060 x g for 15 minutes at 10 °C, pooled and stored at −20 °C before freeze drying and shipping to the NIOZ for lipidome analysis.

Lipidome analysis

The cells of three representative *Sulfurimonas* species (*Ca. S.* marisnigri SoZ1, *Ca. S.* baltica GD2 and *S. gotlandica* GD1^T) were collected and freeze dried for lipidome analysis. A detailed description of sample extraction and ultra-high performance liquid chromatography coupled to high-resolution tandem mass spectrometry (UHPLC-HRMS^2) analysis and initial data processing is given in Bale, et al. [35]. Briefly, freeze-dried samples were extracted using a modified Bligh-Dyer procedure. They were extracted ultrasonically for 10 min, twice in a mixture of methanol, dichloromethane and phosphate buffer (2:1:0.8, v-v:v) and twice with a mixture of methanol, dichloromethane and aqueous trichloroacetic acid solution (TCA) pH 3 (2:1:0.8, v-v:v). The organic phase was separated by adding additional dichloromethane and buffer to a final solvent ratio of 1:1:0.9 (v:v) and were re-extracted three times with dichloromethane and dried under a stream of N_2 gas. The extract was redissolved in a mixture of MeOH:DCM (9:1, v-v) and were filtered through 0.45 μm regenerated cellulose syringe filters (4 mm diameter; Grace Alltech). The extracts were then analyzed using Agilent 1290 Infinity I UHPLC coupled to a Q Exactive Orbitrap MS (Thermo Fisher Scientific, Waltham, MA). The output data files generated by the UHPLC-HRMS^2 analyses were further processed using MZmine software [36]. Process steps included mass peak detection, chromatogram building and deconvolution, isotope grouping, ion component alignment and gap filling [34]. The relative abundance of components was obtained after processing and the combined dataset of MS/MS spectra were analyzed using the Feature Based Molecular Networking tool [33] through the Global Natural Product Social Molecular Networking (GNPS) platform [34] to build molecular networks of the detected components in the dataset (https://gnps.ucsd.edu/ProteoSAFe/status.jsp?task=f775f785684e4cc1b9e133d7abcc6f00). Details can be found in Ding, et al. [37]. It should be noted that many of the lipids detected in this study have not been described previously and hence authentic standards for absolute quantification are not available. Therefore, the lipid compositions were examined in terms of their peak area response. Thus, the relative peak area does not necessarily reflect the actual relative abundance of the different lipids, however, this method allows for some comparison between the samples analyzed in this study. Due to the extraction and analytical methods, and based on annotation from Ding, et al. [37], most of the ion components from the molecular network we generated were lipids and contaminants, thus we used the term "lipidome" for parts of the results and discussion where the lipids are discussed.

RESULTS AND DISCUSSION

Lipidome of three representative *Sulfurimonas* species

Three representative *Sulfurimonas* species were cultured with thiosulfate using NO_3^- or MnO_2 as electron acceptors. Thiosulfate was used instead of HS^- as it is a more convenient electron donor, being non-toxic even in higher concentrations,

and non-reactive with the MnO_2 [13]. Cells were harvested after 12 days of growth, which corresponds to the late exponential or early stationary phase [17]. The growth stages of *Ca*. S. marisnigri SoZ1 and *Ca*. S. baltica GD2 were comparable due to the reliable change in color of the growth media in the late exponential growth phase, and the fact that the time needed to reach final cell densities with NO_3^- does not differ from that with MnO_2 based on our experience with these strains. Similar to the previous studies, growth yields of *Ca*. S. marisnigri SoZ1 and *Ca*. S. baltica GD2 cultured with NO_3^- were substantially lower compared to cultivation with MnO_2 as terminal electron acceptor [17]. The biomass yield of *Ca*. S. marisnigri SoZ1 grown with NO_3^- was too low for a precise lipidomic analysis, therefore it is excluded for the following analysis. *S. gotlandica* GD1^T is unable to grow with MnO_2 [17]. Since only *Ca*. S. baltica GD2 could be cultured with both NO_3^- and MnO_2 conditions, this is the only species that could be examined in terms of its membrane adaptation to a change in electron acceptor. The results of *Ca*. S. marisnigi SoZ1 grown with MnO_2 and *S.* gotlandica GD1 grown with NO_3^- provide complementary information about their lipid specificities and are thus interesting for comparison.

Recently, we established a workflow that provides a substantially expanded view of the molecular composition of the microbial lipidome in environmental settings [37]. Here we used the same workflow for our culture lipidome analysis. The complete dataset produced by analysis with high performance liquid chromatography coupled to high resolution tandem mass spectrometry (HPLC–HRMS^2) of the Bligh-Dyer lipid extracts of the cultures contained 9936 unique ion components, of which 4282 ion components (43%) occurred in structure-similarity groupings in the molecular network, while 5654 ion components occurred as singletons (i.e., components without molecular relatives). A search in the Global Natural Products Social Molecular Networking (GNPS) library [34] resulted in only 167 spectral annotations (<2%). Other than ca. 20 contaminants (e.g., plasticizers), the majority of these annotations were those of well-known glycerol-based lipids: phosphatidylethanolamines (PE-DAGs), phosphatidyl glycerols (PG-DAGs) and triacylglycerols (TAGs). However, the vast majority of ion components was left unannotated. Lipidome annotation remains a bottleneck in marine microbiology lipidomic studies because public databases in this field are poorly populated [35, 37].

The major lipid classes detected in the *Sulfurimonas* spp. were PE/PG-DAGs, diacylglycerols (DAGs) and acyl ether glycerols (AEGs) without a polar head group, ornithine lipids, isoprenoidal quinones, long-chain fatty acids and some unknown lipids (Fig. 1A). The distribution of major lipid classes, based on the peak intensity, were similar between Ca. S. baltica GD2, grown with NO_3^- and with MnO_2 (Fig. 1B). PE/PG-DAGs were dominant among all the lipids, accounting for >80% of total lipids. AEGs were the second most abundant lipid class, accounting for nearly 8% of total lipids. Isoprenoid quinones and some unknown lipids accounted for 0.5–3% of total lipids. PE/PG-DAGs were also the most abundant group of lipids in *Ca*. S. marisnigi SoZ1 grown with MnO_2, comprising 62% of the total lipids, followed by 15% AEGs and 11% unknown lipids. In contrast to Ca. S. baltica GD2 and *Ca*. S. marisnigi SoZ1, PE/PG-DAGs comprised only 39% of total lipids in *S. gotlandica* GD1^T grown with NO_3^-. Ornithine lipids were almost exclusively produced by *S. gotlandica* GD1^T grown with NO_3^- (Fig. S2), accounting for 40% of the total lipids. Ornithine lipids are phosphorus-free amino intact polar lipids. which are relatively common in bacteria, but are absent in eukaryotes and archaea [38]. About 50% of sequenced bacteria are suggested to be able to synthesize ornithine lipids under certain growth conditions [24, 39].

The lipidome differences between Ca. S. marisnigri SoZ1 and S. gotlandica GD1 may be attributed to membrane differences between the species or to factors such as differences in the growth media. Differences in the lipidome of Ca. S. baltica GD2, depending on whether they were grown with NO_3^- or MnO_2, are not evident from the total lipid distribution, so we subsequently examined the compositional differences within specific lipid classes.

PE-DAGs and PG-DAGs are the major components of most bacterial membranes [40, 41] and this also holds for the investigated *Sulfurimonas* species (Fig. 2B). A subnetwork of diverse PE- and PG-DAGs (Fig. 2A) was shown in the molecular network. The acyl moieties (i.e., derived from the esterified fatty acids) of these abundant PEs and PGs had 0–3 double bond equivalents (DBEs) and contained 26–36 carbon atoms (i.e., the sum of the two acyl chains). The majority (i.e., 50–70%) of the PE- and PG-DAGs had 30–32 total acyl carbons with 0 to 2 DBEs. The most dominant individual PE- and PG-associated fatty acids were C_{14}, C_{15} and C_{16}, saturated and monounsaturated fatty acids, in agreement with a previous study that reported that the dominant fatty acid of *S. gotlandica* GD1^T was $C_{16:1}$ (66% of total), with smaller amounts of $C_{18:1}$ and $C_{16:0}$ fatty acids [30]. Our detailed analyses revealed a minority of smaller PE- and PG-DAGs, containing 26–29 total acyl carbons and with 0–1 DBEs. In the only *Sulfurimonas* species that was cultivatable under both NO_3^- and MnO_2 conditions, i.e., *Ca. S.* baltica GD2, the proportion of these smaller PE- and PG-DAGs (26–29 acyl carbons, 0–1 DBEs) was 5.5% of total PE/PG-DAGs under NO_3^- conditions and 17.0% under MnO_2 conditions, suggesting a phospholipid acyl chain adaption in *Ca. S.* baltica GD2 depending on the electron acceptor used.

Novel lipids found in the *Sulfurimonas* species

A subnetwork (>60 components; Fig. 3A, B) entirely populated by unknown lipids (labeled "unknown1" in Fig. 1) revealed a clear division between *Ca*. S. baltica GD2 grown with either NO_3^- or with MnO_2 as the electron acceptor. The composition of this unknown lipid network was also noticeably different between *Ca*. S. marisnigi SoZ1 grown with MnO_2 and *S*. gotlandica GD1 grown with NO_3^-. One of the central and relatively abundant nodes, with a lipid structure occurring in all *Sulfurimonas* spp. grown with NO_3^- or with MnO_2, represents a compound with a molecular ion at *m/z* 771.5657 (as per the molecular network, cf. Fig. 3) eluting at 17.0–17.5 min (Fig. S3). This component was assigned an elemental composition (EC) of $C_{42}H_{80}O_8N_2P^+$ (Δmmu = 1.00; the difference in millimass; [calculated mass – observed mass] x 1000). Upon MS^2 fragmentation (Fig. 3C) a dominant fragment ion at *m/z* 225.1000 with an EC of $C_7H_{18}O_4N_2P^+$ (Δmmu = 0.13) was formed, likely representing the polar headgroup, and a relatively minor and complimentary fragment at *m/z* 547.4704 (EC $C_{35}H_{63}O_4^+$; Δmmu = −1.59) representing the diacyl glycerol core containing the esterified fatty acids with a combined total number of carbon atoms of 32 and 2 DBEs. A single fragment ion at *m/z* 237.2208 with EC of $C_{16}H_{29}O^+$ suggests the diacyl glycerol is composed of two $C_{16:1}$ fatty acids. An apparent loss of H_3PO_4 from the main headgroup ion at *m/z* 225.1000 results in a fragment ion at *m/z* 127.1234, (EC $C_7H_{15}N_2^+$; Δmmu = 0.42) and a further loss of N_2H_2, suggesting the two nitrogen are adjacent to each other in the molecule, results in a fragment ion at *m/z* 97.1012 with an EC of $C_7H_{13}^+$ (Δmmu = −0.52). We, therefore, tentatively identify this lipid as a $C_{16:1}/C_{16:1}$ phosphatidyldiacylglycerol bound to a diazoheptane moiety. The dominance of the fragment ion representing the headgroup in the MS^2 spectrum is very similar to the MS^2 behavior of polar headgroups with a quaternary ammonium (*i.e.*, phosphocholine headgroups) and we, therefore, suggest the diazoheptane moiety is bound not via the terminal N, but to the adjacent N resulting in a quaternary ion. The extracted ion chromatogram of *m/z* 771.5667 (as per the molecular network, cf. Fig. 3) revealed several additional peaks at 18.2–18.5 min (Fig. S3) in the *Sulfurimonas* species grown with

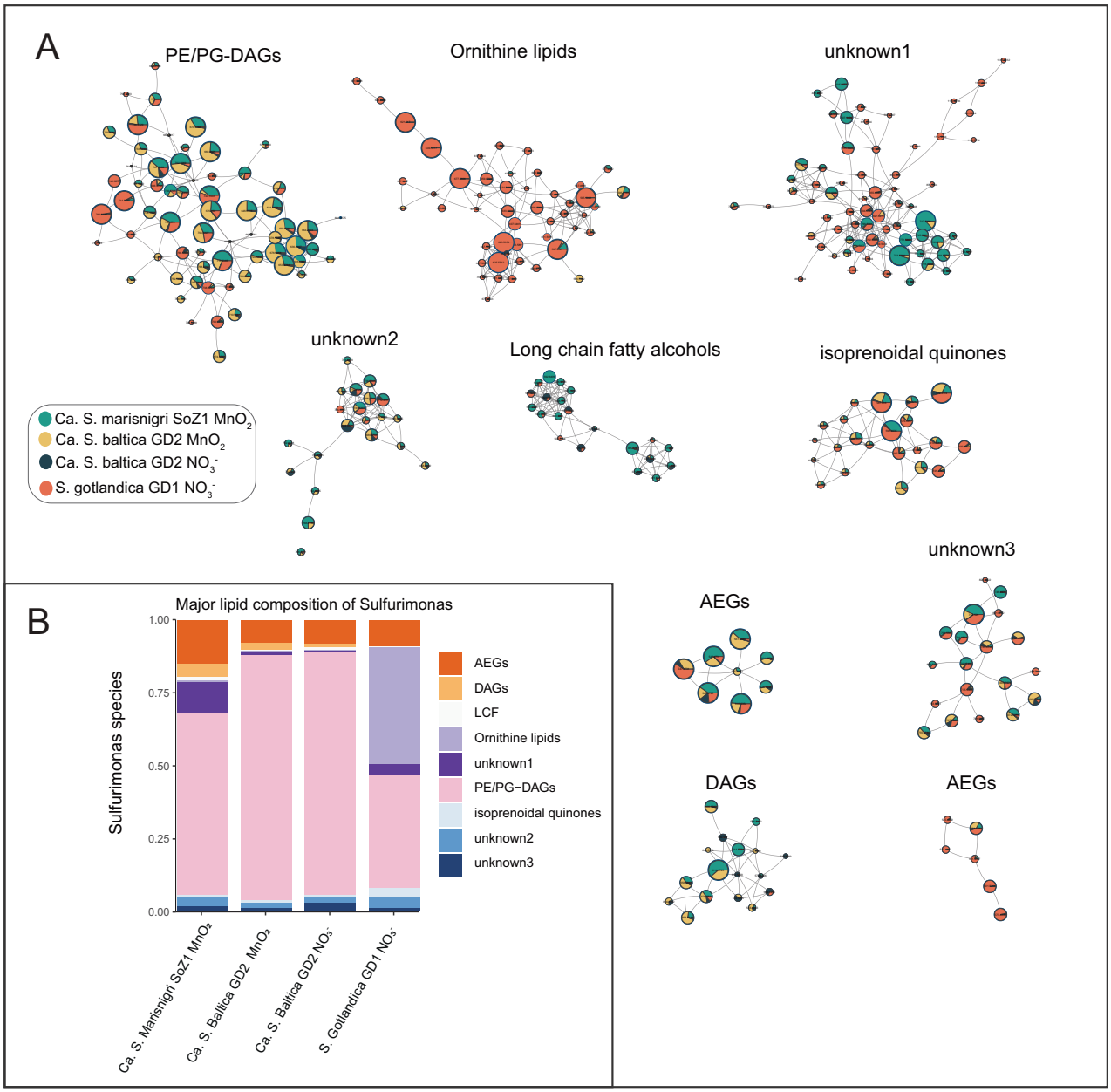

Fig. 1 **A** Molecular network of the major lipid classes in the *Sulfurimonas* species (*Ca. S.* marisnigri SoZ1, *Ca. S.* baltica GD2 and *S. gotlandica* GD1^T) using NO_3^- or MnO_2 as electron acceptors. Nodes represent MS/MS spectra of ion components (lipids), which are connected based on spectral similarity (cosine > 0.6). Nodes are filled with pie charts which contain four different colors representing the fractional abundance of the lipid (based on peak intensity) among three *Sulfurimonas* species with two different treatments. The size of each pie charts represents for the summed intensity of the ion component in all the species using various electron acceptors. The aim of this figure is not to compare the abundance of lipids among different *Sulfurimonas* species, rather than that it provides information on whether specific *Sulfurimonas* spp. under certain conditions have the ability to synthesize specific lipids. The spatial orientation of the nodes in the MS/MS network is randomly generated by Cytoscape [58, 59] and does not relate to relationships between the subnetworks. Lipid classes (clusters) with annotation are either tentatively identified in this study or have been annotated from the GNPS library (see the method for details). **B** Major lipid class composition (based on peak intensity). DAG diacylglycerol, AEG acyletherglycerol, LCF long chain fatty acids, PE phosphatidylethanolamine, PG phosphatidylglycerol. There are also three unknown lipid classes, the structure of unknown lipid 1 will be discussed in Fig. 3. The other two lipid classes are lipids with polar headgroups that we could not identify based on their mass spectra. However, their mass spectra indicate that they comprise a DAG core (Fig. S1).

MnO_2 with identical *m/z* and assigned EC. Interestingly, their fragmentation mass spectrum showed a similar pattern as described for the peak at 17.0–17.5 min (Fig. 3C), however the fragment ion representing the headgroup was now observed at *m/z* 197.0687 (Δmmu = −0.39) and the fragment ion related to the carbon chain in the hydrazine moiety was observed at *m/z* 69 with an EC of $C_5H_9^+$. The fragment ion representing the diacyl core was now observed at *m/z* 575.5038 ($C_{37}H_{67}O_4^+$). In addition to a fragment indicating a $C_{16:1}$ fatty acid, an additional fragment was observed at *m/z* 265 representing a $C_{18:1}$ fatty acid. We therefore assigned this lipid as a phosphatidyldiazopentane diacylglycerol (16:1/18:1). Further inspection of the subnetwork revealed a series of diazoalkyl lipids varying both in the carbon number of the alkylhydrazine headgroup moiety

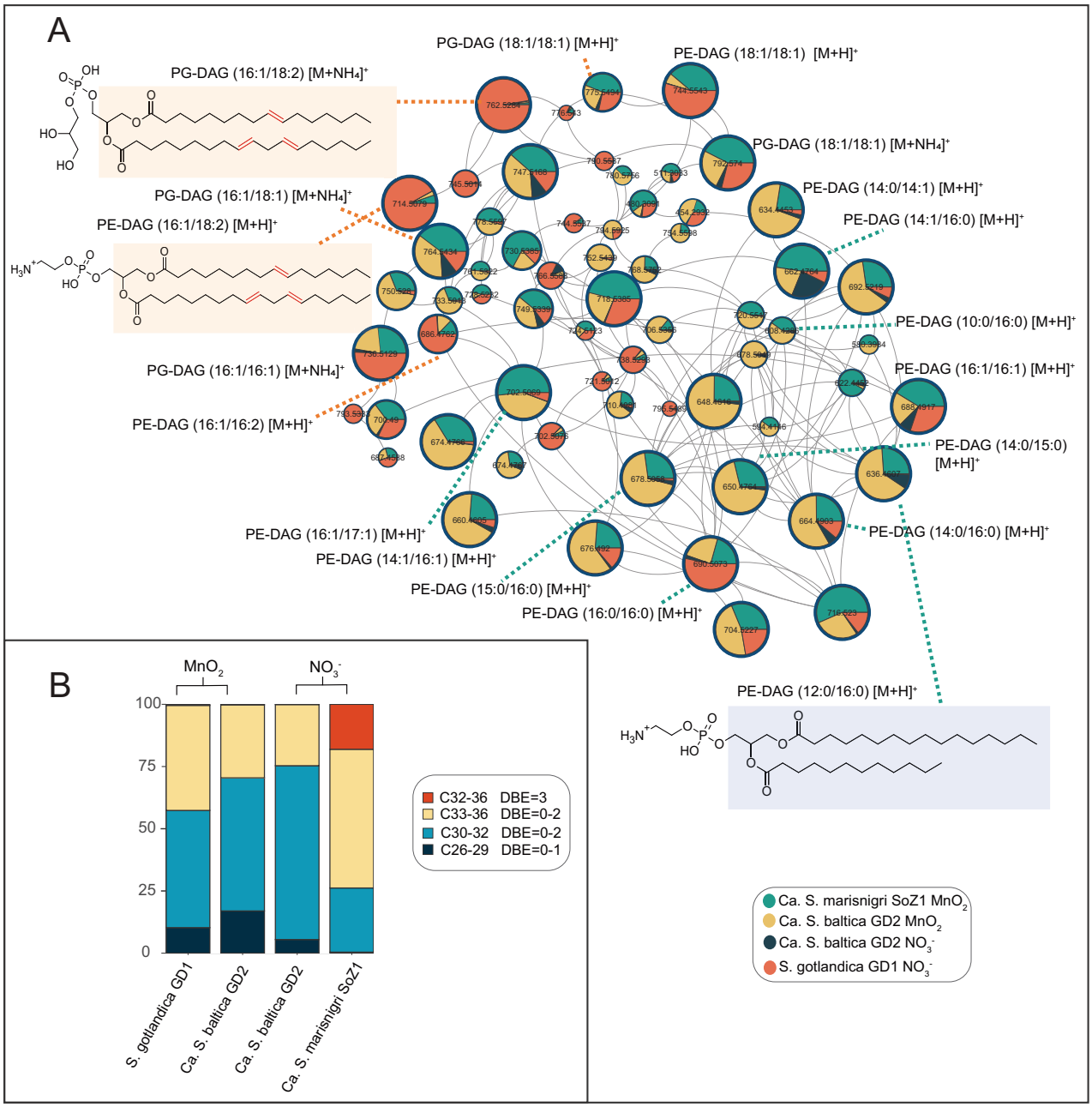

Fig. 2 **A** Molecular subnetwork of PE-DAGs and PG-DAGs. Pie charts shown in the subnetwork are the same as nodes shown in Fig. 1, representing fractional abundance of different individual lipids. The size of the pie charts represents the summed intensity of the ion component in all the species grown with various electron acceptors. Colors of the pie chart represent the fractional abundance of this ion component among all the *Sulfurimonas* species and different treatment. Numbers in the pie charts are the precursor mass of the lipids. Double bonds of the lipid structure are localized tentatively to show their numbers rather than their exact position.; **B** PE-DAG and PG-DAG lipids and their fractional abundance (of total PE-DAGs and PG-DAGs in %) shown in subnetwork of Fig. 2A. The numbers in the labels stand for the total number of carbon atoms of the two acyl chains (C26–36) and their summed double bonds (DBE = 0–3).

from 5 to 11 and in their acyl carbon atoms from 34 to 36, leading to their tentative assignment as phosphatidyldiazoalkyl-diacylglycerols (hereafter, PDA-DAGs). The structural identification here is tentative, further structural elucidation methods (e.g., nuclear magnetic resonance [NMR] spectroscopy) would be required to confirm the proposed structures and elucidate the position of the various functional groups.

The PDA-DAGs with a short C5 alkyl chain in the headgroup were dominant in the two cultures that used MnO_2 as the electron acceptor: Ca. S. marisnigri (90% of total PDA-DAGs) and Ca. S. baltica (74% of total PDA-DAGs) (Fig. 3B). In contrast, Ca. S. baltica GD2, grown with NO_3^-, produced much less C_5 PDA-DAGs (27% of total PDA-DAGs), and mostly C_7 PDA-DAGs, (73%) suggesting a membrane lipid adaptation depending on electron acceptors of this *Sulfurimonas* species. S. gotlandica GD1, unable to grow with MnO_2 as electron acceptor, produced predominantly PDA-DAGs with a headgroup containing a longer alkyl chain (C7 and C11; 49% and 51% of total PDA-DAGs, respectively), while C_5 PDA-DAGs were almost absent (0.1%). The PDA-DAGs composition of Ca. S. marisnigi SoZ1 grown with MnO_2 and on S. gotlandica GD1 grown with NO_3^- were potentially attributed to their species specificities.

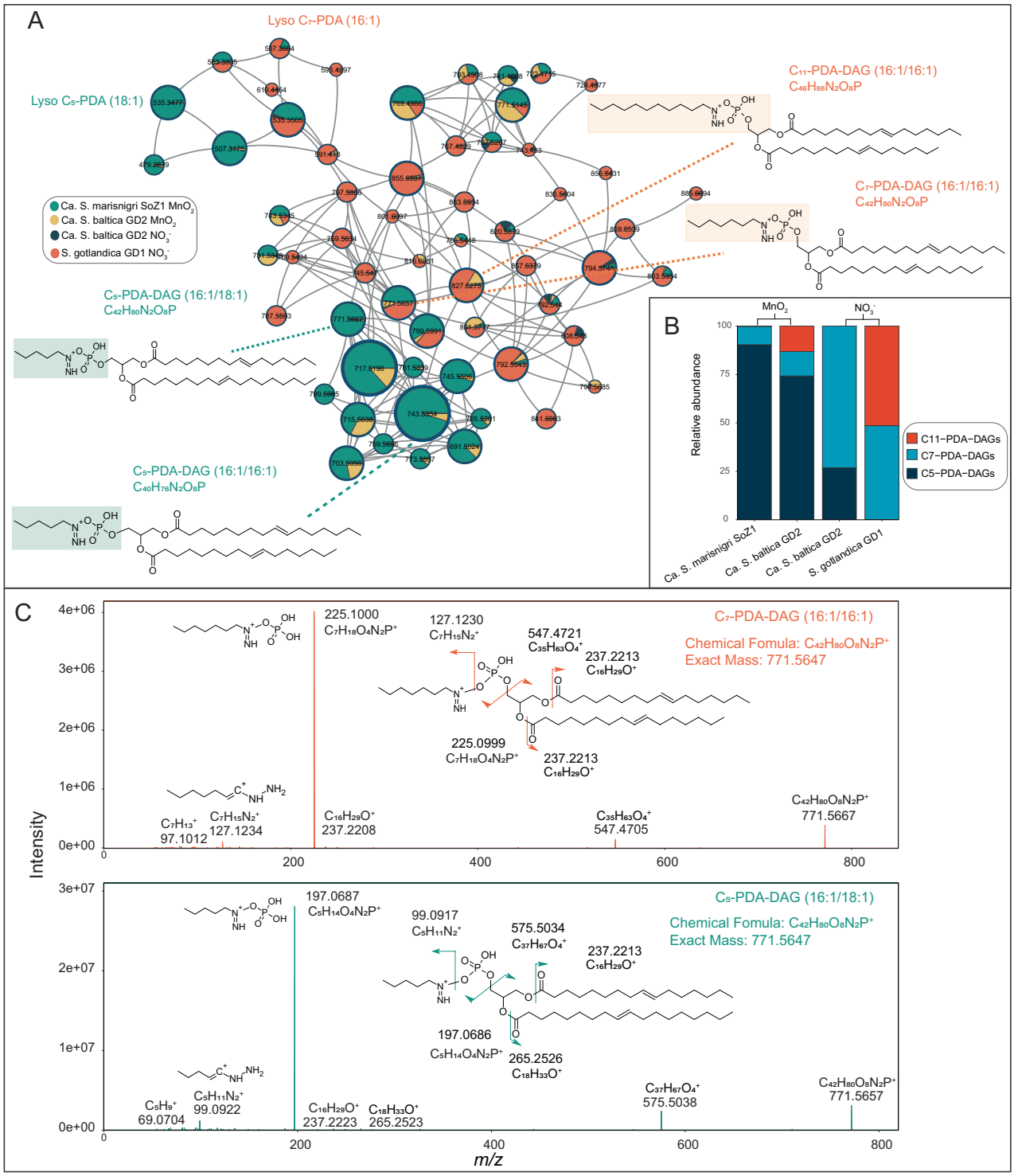

Fig. 3 **A** The molecular subnetwork of the tentatively identified PDA-DAG lipids. Pie charts shown in subnetwork are the same as nodes shown in Fig. 1, representing different lipid structures. The size of the pie charts represents the summed intensity of all the species using various electron acceptors. Colors of pie chart represents the fractional abundance of this lipid among all the *Sulfurimonas* species grown at various conditions. **B** PDA-DAG lipid structures and their fractional abundance of total PDA-DAGs found in subnetwork Fig. 3. **C** MS^2 spectra of two PDA-DAGs that have the same elemental composition (EC of $C_{42}H_{80}O_8N_2P^+$; *m/z* 771.5647) but differ in the size of the alkyl chains of the polar headgroup and the number of carbon atoms of the acyl moieties.

A search using the Mass Spectrometry Search Tool (MASST) of over 1000 public LC-MS datasets available in the GNPS platform database (including lipidomes, metabolomes etc.) was performed to see whether lipids structurally similar to the PDA-DAGs detected in this study of *Sulfurimonas* cultures had been detected in other organisms or environments [34, 37]. However, none of the databases showed matches to these unique lipids, suggesting that either it was due to a database bias or these novel components are potentially indicative of this taxonomic group, because of their specific metabolism or

the environmental adaptation to their niche (redoxcline). Indeed, natural products containing a diazo group are rare [42–44] and their presence in the headgroups of microbial membrane lipids has not been reported before to the best of our knowledge. Although their structure remains tentative, one could speculate about their potential biosynthesis. There are enzymes reported that convert an amine group into a diazo functional group [42]. Primary alkyl amines can be enzymatically produced from fatty acids [45] or by decarboxylation of aliphatic amino acids [46]. The only truly enigmatic biochemical reaction would be the coupling of the diazo functional group with the phosphate moiety of the intact polar lipids.

Potential causes for membrane lipid adaptation with different electron acceptors

Our results revealed marked changes in the composition of (i) the short alkyl chain of the headgroup of PDA-DAG lipids and (ii) the acyl moieties of the PE- and PG-DAGs of *Ca*. S. baltica GD2 depending on the available terminal electron acceptor. It is well established from culture studies that temperature, pressure, pH, growth rate and nutrients are key factors in regulating the fatty acid and headgroup composition of membrane lipids of microorganisms [47–50]. In order to maintain membrane fluidity and permeability at the cultured conditions where pressure is elevated and temperature is low, microorganisms modify their fatty acid composition by increasing the amount of unsaturation and decreasing the chain lengths [21, 51, 52]. Such phenomena were also observed in the natural environment such as the ocean and global soils [53–55]. However, in studies of the eastern subtropical South Pacific, it has been shown that the chain length and degree of unsaturation can be an inherent biochemical property of a lipid class, rather than a function of temperature or pressure [56]. The sequential utilization of terminal electron acceptors is a function of potential energy yield based on thermodynamics which results in the mostly vertically progressive depletion of electron acceptors from O_2 to NO_3^-, Mn(IV), Fe(III) and SO_4^{2-} [57]. Our results suggest that *Ca*. S. baltica GD2 produces shorter chain length lipids when using MnO_2 instead of NO_3^- for energy production. This may indicate that *Ca*. S. baltica GD2 modify their membrane permeability by changing their lipid composition to achieve electron exchange under MnO_2 conditions or due to the different membrane proteins associated with lipids mediating these reactions. To our knowledge, this is the first report of changes in the microbial membrane lipid composition in response to different electron acceptors. Further studies are required to screen for the presence of PDA-DAGs in the natural environment and to determine the biological mechanisms underlying their presence in *Sulfurimonas*.

CONCLUSION

This study showed that the membrane lipid composition of a *Sulfurimonas* species, *Ca*. S. baltica GD2, depends on the electron acceptor used during culturing, either NO_3^- or MnO_2. Differences in the lipid composition of other two species, *Ca*. S. marisnigi SoZ1 grown with MnO_2 and on *S*. gotlandica GD1 grown with NO_3^- were likely attributed to their species specificities. A range of novel diazoalkyl phospholipids were tentatively identified by using molecular network and high-resolution mass spectrometry. We observed that when carrying out MnO_2-dependent sulfur oxidation, *Ca*. S. baltica GD2 possesses shorter acyl (fatty acid) chain lengths in its PE- and PG-DAGs and shorter alkyl chains in its phosphatidyldiazoalkyl-diacylglycerols lipid polar headgroups, compared to the ones produced when grown with NO_3^-. These chain length modifications may be utilized by the cells to maintain membrane homeostasis when using MnO_2 instead of NO_3^- for energy production. Advances in untargeted lipidomic approaches and the development of computational tools will enable the more-efficient characterization of microbial lipidome and the search for unknowns, leading to a better understanding of their functions and metabolism under different environmental conditions.

DATA AVAILABILITY

The HPLC-MS/MS datasets generated during the current study are available from the corresponding author on reasonable request.

REFERENCES

1. Waite DW, Vanwonterghem I, Rinke C, Parks DH, Zhang Y, Takai K, et al. Comparative genomic analysis of the class *Epsilonproteobacteria* and proposed reclassification to Epsilonbacteraeota (phyl. nov.). Front Microbiol. 2017;8:682.
2. Waite DW, Vanwonterghem I, Rinke C, Parks DH, Zhang Y, Takai K, et al. Addendum: Comparative genomic analysis of the Class *Epsilonproteobacteria* and proposed reclassification to Epsilonbacteraeota (phyl. nov.). Front Microbiol. 2018;9:772.
3. Han Y, Perner M. The globally widespread genus *Sulfurimonas*: versatile energy metabolisms and adaptations to redox clines. Front Microbiol. 2015;6:989.
4. Lavik G, Stührmann T, Brüchert V, Van der Plas A, Mohrholz V, Lam P, et al. Detoxification of sulphidic African shelf waters by blooming chemolithotrophs. Nature. 2009;457:581–4.
5. Grote J, Labrenz M, Pfeiffer B, Jost G, Jürgens K. Quantitative distributions of *Epsilonproteobacteria* and a *Sulfurimonas* subgroup in pelagic redoxclines of the central Baltic Sea. Appl Environ Microbiol. 2007;73:7155–61.
6. Grote J, Schott T, Bruckner CG, Glöckner FO, Jost G, Teeling H, et al. Genome and physiology of a model Epsilonproteobacterium responsible for sulfide detoxification in marine oxygen depletion zones. Proc Natl Acad Sci. 2012;109:506–10.
7. Johnston DT, Gill BC, Masterson A, Beirne E, Casciotti KL, Knapp AN, et al. Placing an upper limit on cryptic marine sulphur cycling. Nature. 2014;513:530–3.
8. Walsh DA, Zaikova E, Howes CG, Song YC, Wright JJ, Tringe SG, et al. Metagenome of a versatile chemolithoautotroph from expanding oceanic dead zones. Science. 2009;326:578–82.
9. Wakeham SG, Amann R, Freeman KH, Hopmans EC, Jørgensen BB, Putnam IF, et al. Microbial ecology of the stratified water column of the Black Sea as revealed by a comprehensive biomarker study. Organic Geochem. 2007;38:2070–97.
10. Jost G, Martens-Habbena W, Pollehne F, Schnetger B, Labrenz M. Anaerobic sulfur oxidation in the absence of nitrate dominates microbial chemoautotrophy beneath the pelagic chemocline of the eastern Gotland Basin, Baltic Sea. FEMS Microbiol Ecol. 2009;71:226–36.
11. Taylor GT, Iabichella M, Ho T-Y, Scranton MI, Thunell RC, Muller-Karger F, et al. Chemoautotrophy in the redox transition zone of the Cariaco Basin: A significant midwater source of organic carbon production. Limnology Oceanogr. 2001;46:148–63.
12. Grote J, Jost G, Labrenz M, Herndl Gerhard J, Jürgens K. *Epsilonproteobacteria* represent the major portion of chemoautotrophic bacteria in sulfidic waters of pelagic redoxclines of the Baltic and Black Seas. Appl Environ Microbiol. 2008;74:7546–51.
13. Henkel JV, Dellwig O, Pollehne F, Herlemann DPR, Leipe T, Schulz-Vogt HN. A bacterial isolate from the Black Sea oxidizes sulfide with manganese(IV) oxide. Proc Natl Acad Sci. 2019;116:12153.
14. Henkel JV, Schulz-Vogt HN, Dellwig O, Pollehne F, Schott T, Meeske C, et al. Biological manganese-dependent sulfide oxidation impacts elemental gradients in redox-stratified systems: indications from the Black Sea water column. The ISME J. 2022;16:1523–33.
15. Herszage J, dos Santos Afonso M, Luther GW. Oxidation of cysteine and glutathione by soluble polymeric MnO_2. Environ Sci Technol. 2003;37:3332–8.
16. Yao W, Millero FJ. Oxidation of hydrogen sulfide by hydrous Fe(III) oxides in seawater. Marine Chem. 1996;52:1–16.
17. Henkel JV, Vogts A, Werner J, Neu TR, Spröer C, Bunk B, et al. *Candidatus* Sulfurimonas marisnigri sp. nov. and *Candidatus* Sulfurimonas baltica sp. nov., thiotrophic manganese oxide reducing chemolithoautotrophs of the class *Campylobacteria* isolated from the pelagic redoxclines of the Black Sea and the Baltic Sea. System Appl Microbiol. 2021;44:126155.
18. Kiebish MA, Han X, Cheng H, Lunceford A, Clarke CF, Moon H, et al. Lipidomic analysis and electron transport chain activities in C57BL/6J mouse brain mitochondria. J Neurochem. 2008;106:299–312.
19. Brügger B. Lipidomics: Analysis of the lipid composition of cells and subcellular organelles by electrospray ionization mass spectrometry. Ann Rev Biochem. 2014;83:79–98.

20. Siliakus MF, van der Oost J, Kengen SWM. Adaptations of archaeal and bacterial membranes to variations in temperature, pH and pressure. Extremophiles. 2017;21:651–70.
21. Sinensky M. Homeoviscous adaptation—A homeostatic process that regulates the viscosity of membrane lipids in *Escherichia coli*. Proc Natl Acad Sci. 1974;71:522–5.
22. Popendorf KJ, Tanaka T, Pujo-Pay M, Lagaria A, Courties C, Conan P, et al. Gradients in intact polar diacylglycerolipids across the Mediterranean Sea are related to phosphate availability. Biogeosciences. 2011;8:3733–45.
23. Martin P, Van Mooy BAS, Heithoff A, Dyhrman ST. Phosphorus supply drives rapid turnover of membrane phospholipids in the diatom *Thalassiosira pseudonana*. The ISME J. 2011;5:1057–60.
24. Geiger O, González-Silva N, López-Lara IM, Sohlenkamp C. Amino acid-containing membrane lipids in bacteria. Progr Lipid Res. 2010;49:46–60.
25. Benning C, Huang ZH, Gage DA. Accumulation of a novel glycolipid and a betaine lipid in cells of *Rhodobacter sphaeroides* grown under phosphate limitation. Arch Biochem Biophys. 1995;317:103–11.
26. Van Mooy BAS, Fredricks HF, Pedler BE, Dyhrman ST, Karl DM, Koblížek M, et al. Phytoplankton in the ocean use non-phosphorus lipids in response to phosphorus scarcity. Nature. 2009;458:69.
27. Sebastián M, Smith AF, González JM, Fredricks HF, Van Mooy B, Koblížek M, et al. Lipid remodelling is a widespread strategy in marine heterotrophic bacteria upon phosphorus deficiency. ISME J. 2016;10:968–78.
28. Wang S, Jiang L, Hu Q, Cui L, Zhu B, Fu X, et al. Characterization of *Sulfurimonas hydrogeniphila* sp. nov., a Novel bacterium predominant in deep-sea hydrothermal vents and comparative genomic analyses of the Genus *Sulfurimonas*. Front Microbiol. 2021;12:626705.
29. Wang S, Jiang L, Liu X, Yang S, Shao Z. *Sulfurimonas xiamenensis* sp. nov. and *Sulfurimonas lithotrophica* sp. nov., hydrogen- and sulfur-oxidizing chemolithoautotrophs within the *Epsilonproteobacteria* isolated from coastal sediments, and an emended description of the genus *Sulfurimonas*. Int J System Evolut Microbiol. 2020;70:2657–63.
30. Labrenz M, Grote J, Mammitzsch K, Boschker HTS, Laue M, Jost G, et al. *Sulfurimonas gotlandica* sp. nov., a chemoautotrophic and psychrotolerant epsilonproteobacterium isolated from a pelagic redoxcline, and an emended description of the genus *Sulfurimonas*. Int J Syst Evolut Microbiol. 2013;63:4141–8.
31. Law KP, Zhang CL. Current progress and future trends in mass spectrometry-based archaeal lipidomics. Organic Geochem. 2019;134:45–61.
32. Collins JR, Edwards BR, Fredricks HF, Van Mooy BAS. LOBSTAHS: an adduct-based lipidomics strategy for discovery and identification of oxidative stress biomarkers. Anal Chem. 2016;88:7154–62.
33. Nothias L-F, Petras D, Schmid R, Dührkop K, Rainer J, Sarvepalli A, et al. Feature-based molecular networking in the GNPS analysis environment. Nat Methods. 2020;17:905–8.
34. Wang M, Carver JJ, Phelan VV, Sanchez LM, Garg N, Peng Y, et al. Sharing and community curation of mass spectrometry data with Global Natural Products Social Molecular Networking. Nat Biotechnol. 2016;34:828–37.
35. Bale NJ, Ding S, Hopmans EC, Arts MGI, Villanueva L, Boschman C, et al. Lipidomics of environmental microbial communities. I: Visualization of component distributions using untargeted analysis of high-resolution mass spectrometry data. Front Microbiol. 2021;12:659302.
36. Pluskal T, Castillo S, Villar-Briones A, Orešič M. MZmine 2: Modular framework for processing, visualizing, and analyzing mass spectrometry-based molecular profile data. BMC Bioinformatics. 2010;11:395.
37. Ding S, Bale NJ, Hopmans EC, Villanueva L, Arts MGI, Schouten S, et al. Lipidomics of environmental microbial communities. II: Characterization using molecular networking and information theory. Front Microbiol. 2021;12:659315.
38. Vences-Guzmán MÁ, Geiger O, Sohlenkamp C. Ornithine lipids and their structural modifications: from A to E and beyond. FEMS Microbiol Lett. 2012;335:1–10.
39. Sohlenkamp C, Geiger O. Bacterial membrane lipids: diversity in structures and pathways. FEMS Microbiol Rev. 2016;40:133–59.
40. Raetz C, Dowhan W. Biosynthesis and function of phospholipids in *Escherichia coli*. J Biol Chem. 1990;265:1235–8.
41. Gill C. Effect of growth temperature on the lipids of *Pseudomonas fluorescens*. Microbiology. 1975;89:293–8.
42. Nawrat CC, Moody CJ. Natural products containing a diazo group. Nat Product Rep. 2011;28:1426–44.
43. Sugai Y, Katsuyama Y, Ohnishi Y. A nitrous acid biosynthetic pathway for diazo group formation in bacteria. Nat Chem Biology. 2016;12:73–75.
44. Chen L, Deng Z, Zhao C. Nitrogen–nitrogen bond formation reactions involved in natural product biosynthesis. ACS Chem Biology. 2021;16:559–70.
45. Anderson R, Huang Y. Fatty acids are precursors of alkylamines in *Deinococcus radiodurans*. J Bacteriol. 1992;174:7168–73.
46. Kim DI, Chae TU, Kim HU, Jang WD, Lee SY. Microbial production of multiple short-chain primary amines via retrobiosynthesis. Nat Commun. 2021;12:173.
47. Wada H, Gombos Z, Murata N. Contribution of membrane lipids to the ability of the photosynthetic machinery to tolerate temperature stress. Proc Natl Acad Sci. 1994;91:4273–7.
48. DeLong EF, Yayanos AA. Adaptation of the membrane lipids of a deep-Sea bacterium to changes in hydrostatic pressure. Science. 1985;228:1101–3.
49. Chwastek G, Surma MA, Rizk S, Grosser D, Lavrynenko O, Rucińska M, et al. Principles of membrane adaptation revealed through environmentally induced bacterial lipidome remodeling. Cell Reports. 2020;32:108165.
50. Vinçon-Laugier A, Cravo-Laureau C, Mitteau I, Grossi V. Temperature-dependent alkyl glycerol ether lipid composition of mesophilic and thermophilic sulfate-reducing bacteria. Front Microbiol. 2017;8:1532.
51. Oshima M, Miyagawa A. Comparative studies on the fatty acid composition of moderately and extremely thermophilic bacteria. Lipids. 1974;9:476–80.
52. Sinensky M. Temperature control of phospholipid biosynthesis in *Escherichia coli*. J Bacteriol. 1971;106:449–55.
53. Fang J, Barcelona MJ, Nogi Y, Kato C. Biochemical implications and geochemical significance of novel phospholipids of the extremely barophilic bacteria from the Marianas Trench at 11,000m. Deep Sea Res Part I: Oceanogr Res Pap. 2000;47:1173–82.
54. Weijers JWH, Schouten S, van den Donker JC, Hopmans EC, Sinninghe, Damsté JS. Environmental controls on bacterial tetraether membrane lipid distribution in soils. Geochimica et Cosmochimica Acta. 2007;71:703–13.
55. Holm Henry C, Fredricks Helen F, Bent Shavonna M, Lowenstein Daniel P, Ossolinski Justin E, Becker Kevin W, et al. Global ocean lipidomes show a universal relationship between temperature and lipid unsaturation. Science. 2022;376:1487–91.
56. Van Mooy BAS, Fredricks HF. Bacterial and eukaryotic intact polar lipids in the eastern subtropical South Pacific: Water-column distribution, planktonic sources, and fatty acid composition. Geochimica et Cosmochimica Acta. 2010;74:6499–516.
57. Jørgensen BB, Findlay AJ, Pellerin A. The biogeochemical sulfur cycle of marine sediments. Front Microbiol. 2019;10:849.
58. Smoot ME, Ono K, Ruscheinski J, Wang P-L, Ideker T. Cytoscape 2.8: new features for data integration and network visualization. Bioinformatics. 2010;27:431–2.
59. Shannon P, Markiel A, Ozier O, Baliga NS, Wang JT, Ramage D, et al. Cytoscape: a software environment for integrated models of biomolecular interaction networks. Genome Res. 2003;13:2498–504.

ACKNOWLEDGEMENTS

Two anonymous referees are thanked for helpful comments and S. Schouten, P. Riekenberg and M.T.J. van der Meer for helpful discussions. We acknowledge A. Abdala, D. Dorhout, J. Ossebaar, M. Verweij, A. Mets for technical support. JSSD received funding from the European Research Council (ERC) under the European Union's Horizon 2020 research and innovation program (grant agreement no. 694569—MICROLIPIDS) and from a Spinoza award from NWO.

AUTHOR CONTRIBUTIONS

SD, JVH, NB, LV, ECH and JSSD conceived the concept. SD carried out the data analyses. JVH cultured organisms. MK carried out the lipid extraction and ECH ran MS experiments. SD, ECH, NB and JSSD performed the lipid identification. SD wrote the initial manuscript with the input of all authors. JSSD and LV supervised the study. All authors edited and approved the final manuscript.

COMPETING INTERESTS

The authors declare no competing interests.

ADDITIONAL INFORMATION

Supplementary information The online version contains supplementary material available at https://doi.org/10.1038/s43705-022-00207-3.

Correspondence and requests for materials should be addressed to Su Ding.

Reprints and permission information is available at http://www.nature.com/reprints

Publisher's note Springer Nature remains neutral with regard to jurisdictional claims in published maps and institutional affiliations.